Collective nature of plasticity in mediating phase transformation under shock compression

Hongxiang Zong,[1,2] Xiangdong Ding,[1,*] Turab Lookman,[2,*] Ju Li,[1,3] Jun Sun,[1] Ellen K. Cerreta,[4] J. P. Escobedo,[4] Francis L. Addessio,[2] and Curt A. Bronkhorst[2]

[1]*State Key Laboratory for Mechanical Behavior of Materials, Xi'an Jiaotong University, Xi'an 710049, China*
[2]*Theoretical Division, Los Alamos National Laboratory, Los Alamos, New Mexico 87545, USA*
[3]*Department of Nuclear Science and Engineering and Department of Materials Science and Engineering, Massachusetts Institute of Technology, Cambridge, Massachusetts 02139, USA*
[4]*Materials Science and Technology Division, Los Alamos National Laboratory, Los Alamos, New Mexico 87545, USA*

An open question in the behavior of metals subjected to shock is the nature of the deformation that couples to the phase transformation process. Experiments to date cannot discriminate between the role of known deformation processes such as twinning or dislocations accompanying a phase change, and modes that can become active only in extreme environments. We show that a deformation mode not present in static conditions plays a dominant role in mediating plastic behavior in hcp metals and determines the course of the transformation. Our molecular dynamics simulations for titanium demonstrate that the transformation is preceded by a 90° lattice reorientation of the parent, and the growth of the reoriented domains is accompanied by the collective action of dislocations and deformation twins. We suggest how diffraction and transmission electron microscopy experiments may validate our findings.

Materials dynamics, particularly the behavior of solids under extreme compression, is a topic of broad scientific and technological interest [1–5]. The shock impulse provides a unique probe to excite and thereby examine the response of materials to dynamic compression. It is well known that if a material undergoes shock compression beyond the Hugoniot elastic limit, it exhibits rapid plastic flow which is expected to occur via the generation and propagation of defects (twin, dislocations, etc.) [1,6–10], and possible phase transformations [11–14]. In the presence of large peak stresses, strain rates, and significant inelastic strain due to shock, these plastic deformation modes can differ from those observed under longer time scales or more quasistatic conditions [1,6], and may interact with the phase transformations [15,16]. However, when solids undergo phase transformations, a key question is how these deformation modes mediate the phase transformation process.

The group-IV hexagonal-close-packed (hcp) metals Zr, Ti, and Hf, with transition temperatures and pressures that are relatively accessible, have served as an excellent test bed for studying aspects of deformation and phase transformation behavior under driven conditions. For the α (hcp) to ω (hexagonal) phase transformation, progress over the last three decades from recovery experiments and analysis of wave profiles [17–19] has largely focused on capturing the behavior of the equation of state, orientation relationships in microstructures, understanding the influence of impurities such as oxygen, and characterizing the deformation. A number of studies have recognized that the plastic flow behavior as a result of the transformation is accompanied by twinning and slip under different loading and temperature conditions [18–20]. However, recovered samples under shock have invariably been for polycrystals and the deformation modes of twinning and

slip have largely been inferred from textural analysis. What has been apparent is that there is twinning or some form of reorientation in samples shocked below the transformation pressure and that the volume fraction of the transformed ω phase is higher at higher peak pressures [17]. Further, electron backscattered diffraction data on Zr polycrystal shows that the ω appears to reside in regions previously twinned or rotated in samples shocked below the transformation pressure and that the reorientation is greater when the fraction of transformed ω is higher (see Supplemental Material, Fig. S1 [21]). Such measurements, although not able to discriminate between twinning and reorientation, especially when the differences can be only a few degrees, are beginning to indicate some form of coexistence of different types or "variants" of the α phase with the ω, and that some form of plastic deformation is mediating the reorientation process within the microstructure.

In this work we show that under shock compression the phase transformation in hcp Ti is preceded by a collective deformation mode. This mode gives rise to new domains or variants, which differ in lattice orientation by 90° compared to the original parent, and do not belong to any known hcp twin systems. This domain reorientation is accompanied by the formation and motion of deformation twins and dislocations that act cooperatively to move the domain boundary. Thus we demonstrate that under shock conditions it is necessary to go beyond conventional ideas of the role of deformation twinning, and dislocation line based slip, a new mode of plasticity, becomes active.

Our nonequilibrium molecular dynamics (NEMD) simulations were performed in a microcanonical ensemble using the LAMMPS code [22]. The interatomic interactions in Ti were described by a modified embedded atom method potential developed in [23,24]. This potential gives accurate total energies, elastic constants, and phonon spectra, as well as reasonable values for point defects and surface and

———————
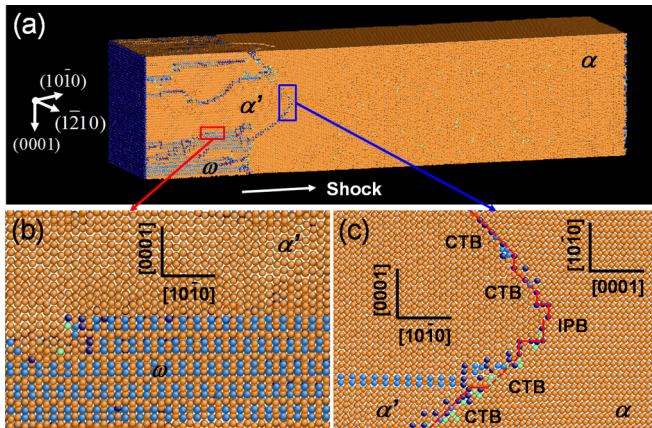*Corresponding author: dingxd@mail.xjtu.edu.cn; txl@lanl.gov

FIG. 1. (Color online) Microstructure from NEMD shock simulations of shocked Ti single crystal samples. (a) Shocked samples with particle velocity, $u_p = 7.5$ m/s along $[10\bar{1}0]$ direction containing approximately 3.0 million atoms in volume 24 nm × 24 nm × 200 nm after 18.0 ps. The initial hcp α phase, reoriented hcp α' phase, and transformed ω phase are shown with a trapezoidal-shaped domain boundary separating α and α'. (b) Coexisting [0001] α' and transformed ω phases. (c) The 90° domain boundary between α and α' from the cross section (blue rectangle) in (a) consists of an IPB, CTBs, and dislocation kinks and disconnections.

stacking fault energies. In addition, our MD simulations (Supplemental Material, Fig. S2 [21]) show that this potential reasonably reproduces the shock Hugoniot for Ti [25]. The z axis of the simulation box was oriented along the $[10\bar{1}0]$ shock direction, with periodic boundary conditions transverse to the shock-wave propagation. The simulations covered up to 0.2-μm-thick single crystal titanium samples, using up to 3.0 million atoms. After isothermally annealing the sample at 30 K for 1.2 ns, the left surface of the system was driven by the piston with a velocity $u_p = 0.75$ km/s and peak pressure 14 GPa, above the threshold piston velocity of 0.57 km/s required to induce a phase change in Ti.

Figure 1(a) is a snapshot after 18 ps of the Ti sample shocked along the $[10\bar{1}0]$ direction. The parent hcp α phase undergoes a rotation to the product α' separated by a trapezoidal-shaped boundary, and the ω phase nucleates within the α' matrix. Figure 1(c) is an enlargement of a part of the boundary showing the orientation relationship between α and rotated α'. The $[10\bar{1}0]$ α (prismatic stacking) that is orientated along the shock direction, rotates to the [0001] α' variant (basal stacking) and these two orientations are separated by a domain boundary. This boundary consists of two types of segments: the $\{10\bar{1}2\}$ coherent twin boundary (CTB) segments, which are the same as the well-known hcp tensile deformation twins, and incoherent prismatic-basal boundaries (IPBs). The latter segments (IPBs) contain dislocations and disconnections or lattice steps. Figure 1(c) shows a section of the domain boundary with the constituent elements above identified. Following the hcp domain rotation, part of the α' phase then converts to ω phase, as shown in Fig. 1(b). Indexing of the thin section of shocked specimen shows that the experimentally observed Silcock orientation relationship [26,27] between α' and ω (rather than *unrotated* α and ω) is obeyed (see Supplemental Material, Fig. S3 [21]).
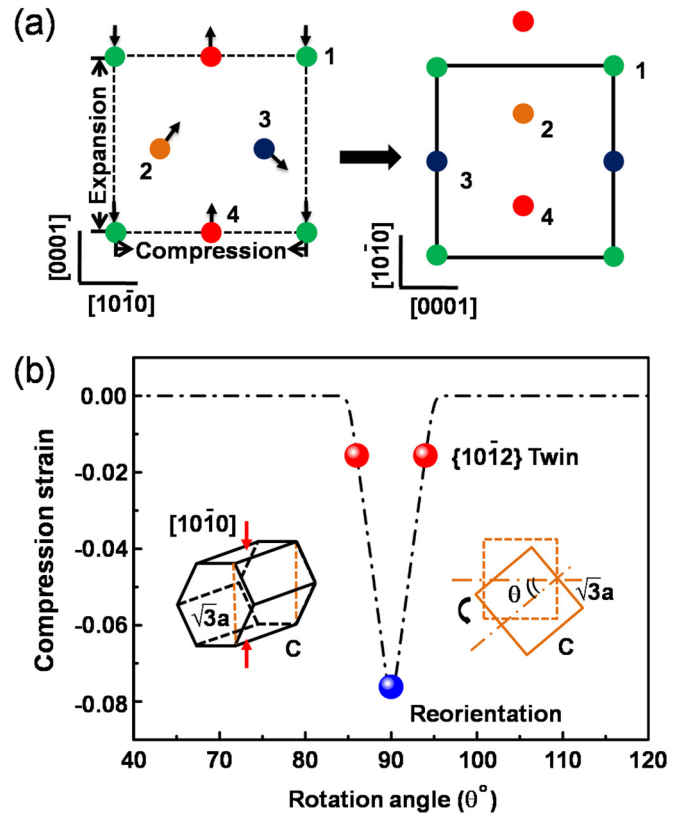

FIG. 2. (Color online) Lattice reorientation from $[10\bar{1}0]$-oriented hcp to [0001]-oriented hcp in terms of a displacive transformation mechanism. (a) The lattice reorientation can be described in terms of a shuffle (displacement) and a global shape change. The arrows show the shuffle directions for the four atoms. (b) Comparison of the compressional strain versus reorientation angles for the 90° reorientation and $\{10\bar{1}2\}$ twins. The left schematic shows compression direction on the hcp unit cell. The $(1\bar{2}10)$ plane shown as a dotted line rotates by angle θ (right schematic). A rotation of 84.6° gives rise to $\{10\bar{1}2\}$ twins and 90° leads to the reoriented domains discussed in this work.

The lattice rotation of 90° across the domain boundary (hereafter referred to as 90° domain boundary) that we have identified does not obey any of the known twin symmetries for hcp. We therefore need a different mechanism to facilitate this crystal reorientation. In pure hcp Ti crystals, the deformation twin modes most commonly reported (under static loading conditions) are $\{10\bar{1}2\}$ and $\{11\bar{2}2\}$ twins [28,29]. The $[10\bar{1}0]$ compression strain as a result of the shock will give rise to the $\{10\bar{1}2\}$ twinning mode with an 84.6° rotation angle between α and α'. This is close to but not the 90° lattice reorientation we observe. Rather, the 90° reorientation process can be expressed as the result of the coupled effects of shear strains and shuffles (or atomic displacements) [see Fig. 2(a)], analogous to the formation of orientational variants in martensitic transformations [11,30]. As Fig. 2(a) indicates, the shear along $\langle 10\bar{1}1 \rangle$ directions rotates the hcp unit cell by 90° via the coupling of a compressional strain along $[10\bar{1}0]$ and a tensile strain along [0001]. Meanwhile, the atomic shuffles (two atoms move along $\langle 10\bar{1}1 \rangle$ and the other two along $\langle 0001 \rangle$ directions) occur as shown by arrows in Fig. 2(a).
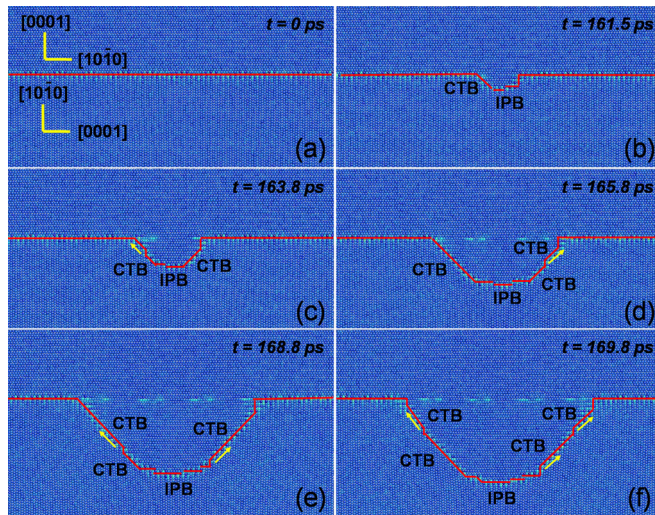
FIG. 3. (Color online) The migration of the 90° domain boundary to accommodate the lattice reorientation process under uniaxial compression. (a) The initial bicrystal between the reoriented α' and the original α matrix. (b) The formation of IPB and coherent {10$\bar{1}$2} twin boundary (CTB). (c)–(f) The incoherent domain boundary motion via collective behavior involving IPB and CTBs. Kinks or twinning dislocations are continually emitted from the junction of IPB and CTB and drive further CTB migration.

The compressive strain (8%) induced by lattice reorientation from [10$\bar{1}$0] to [0001] is much larger than for deformation twinning (2%) [Fig. 2(b)], and is the reason the new mode can be activated under shock compression. The shear and shuffle process give rise to the new reoriented domains of hcp.

The reoriented domains need to be elastically accommodated [31] and this occurs by the generation of dislocations and coherent twin boundaries, which form the interface (90° domain boundary) between the unrotated and rotated regions. In order to gain insight into this process, we simulated a bicrystal of Ti with the same orientation relationship as α and α' [Fig. 3(a)] with a compressive stress acting perpendicular to the domain boundary. The stress direction is therefore the same as the shock direction shown in Fig. 1. After the initial

elastic deformation, the lattice reorientation [a few atomic layers height in Fig. 3(b)] occurs from the initial interface and this leads to the formation of sections of IPBs separated by steps [Fig. 3(b)]. Subsequently, as shown in Figs. 3(b) and 3(c), {10$\bar{1}$2} CTB segments are generated on the wings accompanied by the migration of the IPBs. Thus, a 90° domain boundary consisting of IPBs and CTBs is formed. Under further compression, kinks are emitted from the junctions of IPBs and CTBs, and move along the CTBs causing the CTBs to migrate rapidly along the loading direction [Fig. 3(c)]. When repeated, this process leads to the propagation of the trapezoidal boundary [Figs. 3(d)–3(f); also Supplemental Material, Movie 1 [21]), which is similar to the propagation of the domain boundary as observed in our shock NEMD simulations [Fig. 1(c)]. We note that it is the interaction of the dislocations contained within IPBs with the CTBs that nucleates these kinks, which act as sources of twinning dislocations (or mobile disconnections) facilitating further twin boundary migration (Supplemental Material, Fig. S4 [21]). Thus, extra deformation twin nucleation processes need not be invoked. Our work does have parallels with defective twin boundaries in Cu nanocrystals [32,33] in which kinks act as twin dislocation sources and strongly influence the ductility of nanotwinned materials.

Our aim has been to probe the deformation mechanism mediating the phase transformation process in materials subjected to shock conditions. Experiments on recovered polycrystal shocked samples have only indicated some form of lattice reorientation prior to the transformation, but have not been able to discriminate between twinning and other forms of domain reorientation. In this work, we used atomistic simulations to show that the transformation is preceded by a collective mode that leads to a 90° domain reorientation. This mode involves a combination of deformation twins and dislocations that act to move the domain boundary. It is similar to shear induced grain boundary motion [34–37] where the normal migration of a grain boundary is only coupled to simple shear. In our case, the mode is driven by uniaxial compression. Moreover, it involves a more cooperative or collective movement of a large number of atoms within the prismatic-basal stacking rearrangement, similar to that in a
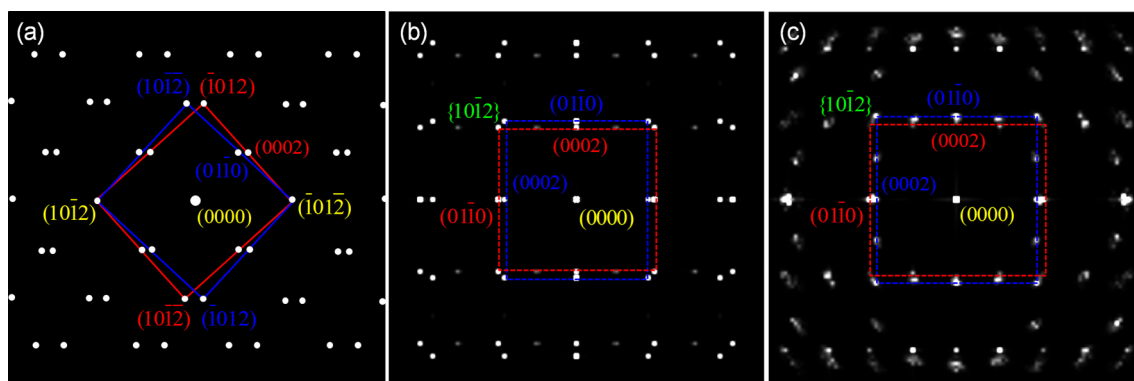

FIG. 4. (Color online) Comparison of diffraction patterns obtained from deformation twinning and 90° domain boundary. (a) The far-field pattern for deformation twins with {10$\bar{1}$2} twin orientation relationship. The two coincident {10$\bar{1}$2} reflections connote a coherent twin boundary. (b) The diffraction pattern of lattice reorientation from an ideal 90° domain boundary [Fig. 3(f)]. Here, all the {10$\bar{1}$2} spots are separated because of the 90° reorientation, (c) as in (b) but from a 90° domain boundary from our simulations [from cross section S in Fig. 1(a)].

martensitic transformationlike. Our work thus suggests that coappearance of transformationlike plastic deformation and phase transformation may be more common under shock than previously assumed. In addition, we note that the observed orientation relationship for the α to ω phase transformation is between the *reoriented* parent phase and the resulting ω phase. The importance of this has not been previously realized and may be verified by transmission electron microscopy (TEM) on shock-recovered samples [18,38].

With the emergence of *in situ* and high resolution temporal and spatial x-ray probes, we have calculated diffraction patterns in the far-field limit. These contain intensities from a plane in reciprocal space being viewed along the zone axis perpendicular to the compression or shock direction. Figures 4(a) and 4(b) compare such diffraction patterns from an ideal {10$\bar{1}$2} deformation twin to a 90° domain boundary for a Ti single crystal [Fig. 3(f)]. The reflections from the twin plane are coincident, indicating that the plane is coherent, whereas for the 90° domain boundary the {10$\bar{1}$2} reflections are separated. The 90° reorientation leaves all off-centered reflections separated. The pattern obtained from the marked region *S* in Fig. 1(a) from our simulations is shown in Fig. 4(c).

The reflections are more diffused compared to Fig. 4(b), but the pattern is similar. Although our calculated patterns are more accessible with TEM, laser pump-probe measurements [39] using an XFEL (for example, at LCLS, SLAC) or measurements at APS on high purity single crystal Ti can potentially provide data on changes in microstructural reorientation. The resolution will sensitively depend on bandwidth, factors such as the initial crystal orientation and setup, all of which will have a bearing on the number of points in reciprocal space satisfying the Bragg condition. LCLS can provide the means to develop an *in situ* "movie" using a time delay on many statistically similar samples and such measurements can validate our predictions by following changes in intensity with time resolutions of subnanoseconds or better.

[1] M. A. Meyers, *Dynamic Behavior of Materials* (Wiley, New York, 1994).

[2] H. E. Lorenzana, J. F. Belak, K. S. Bradley, E. M. Bringa, K. S. Budil, J. U. Cazamias, B. El-Dasher, J. A. Hawreliak, J. Hessler, K. Kadau, D. H. Kalantar, J. M. McNaney, D. Milathianaki, K. Rosolankova, D. C. Swift, M. Taravillo, T. W. Van Buuren, J. S. Wark, and T. Diaz de la Rubia, Sci. Model Simul. **15**, 159 (2008).

[3] T. d'Almeida and Y. M. Gupta, Phys. Rev. Lett. **85**, 330 (2000).

[4] J.-S. Lauret, C. Voisin, G. Cassabois, C. Delalande, P. Roussignol, O. Jost, and L. Capes, Phys. Rev. Lett. **90**, 057404 (2003).

[5] E. J. Reed, M. Soljacic, R. Gee, and J. D. Joannopoulos, Phys. Rev. Lett. **96**, 013904 (2006).

[6] M. A. Meyers, H. Jarmakani, E. M. Bringa, and B. A. Remington, in *Dislocations in Solids*, edited by J. P. Hirth and L. Kubin (Elsevier, New York, 2009), p. 91.

[7] E. M. Bringa, K. Rosolankova, R. E. Rudd, B. A. Remington, J. S. Wark, M. Duchaineau, D. H. Kalantar, J. Hawreliak, and J. Belak, Nat. Mater. **5**, 805 (2006).

[8] T. C. Germann, B. L. Holian, P. S. Lomdahl, and R. Ravelo, Phys. Rev. Lett. **84**, 5351 (2000).

[9] M. J. Suggit, A. Higginbotham, J. A. Hawreliak, G. Mogni, G. Kimminau, P. Dunne, A. J. Comley, N. Park, B. A. Remington, and J. S. Wark, Nat. Commun. **3**, 1224 (2012).

[10] M. W. Chen, J. W. McCauley, D. P. Dandekar, and N. K. Bourne, Nat. Mater. **5**, 614 (2006).

[11] K. Kadau, T. C. Germann, P. S. Lomdahl, and B. L. Holian, Science **296**, 1681 (2002).

[12] G. T. Gray, III, Annu. Rev. Mater. Res. **42**, 285 (2012).

[13] P. S. Branicio, R. K. Kalia, A. Nakano, and P. Vashishta, Phys. Rev. Lett. **96**, 065502 (2006).

[14] G. E. Duval and R. A. Graham, Rev. Mod. Phys. **49**, 523 (1977).

[15] D. E. Grady, J. Geophys. Res. **84**, 7549 (1979).

[16] B. W. Dodson and E. L. Venturini, *Shock Waves in Condensed Matter*, AIP Conf. Proc. No. 78 (AIP, Melville, NY, 1982), p. 335.

[17] E. Cerreta, G. T. Gray, III, R. S. Hixson, P. A. Rigg, and D. W. Brown, Acta Mater. **53**, 1751 (2005).

[18] S. G. Song and G. T. Gray III, Philos. Mag. A **71**, 275 (1995).

[19] E. K. Cerreta, G. T. Gray, C. P. Trujillo, D. W. Brown, and C. N. Tomé, *Shock Waves in Condensed Matter*, AIP Conf. Proc. No. 955 (AIP, Melville, NY, 2007), p. 635.

[20] N. K. Bourne, G. T. Gray III, and J. C. F. Millett, J. Appl. Phys. **106**, 091301 (2009).

[21] See Supplemental Material at http://link.aps.org/supplemental/10.1103/PhysRevB.89.220101 for Zr polycrystalline shock experimental setup details and results, a description of the MD simulation results of shock Hugoniot for Ti, transformation pathway, a movie of 90° domain boundary migration, as well as the interaction mechanism between dislocation arrays and CTBs.

[22] S. Plimpton, J. Comput. Phys. **117**, 1 (1995).

[23] T. J. Lenosky, B. Sadigh, E. Alonso, V. V. Bulatov, T. D. de la Rubia, J. Kim, A. F. Voter, and J. D. Kress, Modell. Simul. Mater. Sci. Eng. **8**, 825 (2000).

[24] D. R. Trinkle, *A Theoretical Study of the hcp to Omega Martensitic Phase Transition in Titanium* (The Ohio State University, Columbus, 2003).

[25] S. P. Marsh, *Lasl Shock Hugoniot Data* (University of California Press, Berkeley, 1980).

[26] J. M. Silcock, Acta Metall. **6**, 481 (1958).

[27] R. Kutsar, I. V. Lyasotski, A. M. Podurets, and A. F. Sanches-bolinches, High Press. Res. **4**, 475 (1990).

[28] M. Battaini, E. V. Pereloma, and C. H. J. Davies, Metall. Mater. Trans. A **38**, 276 (2007).

[29] D. R. Chichili, K. T. Ramesh, and K. J. Hemker, Acta Mater. **46**, 1025 (1998).

[30] D. H. Kalantar, J. F. Belak, G. W. Collins, J. D. Colvin, H. M. Davies, J. H. Eggert, T. C. Germann, J. Hawreliak, B. L. Holian, K. Kadau, P. S. Lomdahl, H. E. Lorenzana, M. A. Meyers, K. Rosolankova, M. S. Schneider, J. Sheppard, J. S. Stolken, and J. S. Wark, Phys. Rev. Lett. **95**, 075502 (2005).

[31] Ekhard K. H. Salje, Annu. Rev. Mater. Res. **42**, 265 (2012).

[32] J. W. Yan, X. F. Zhu, B. Yang, and G. P. Zhang, Phys. Rev. Lett. **110**, 155502 (2013).

[33] Y. M. Wang, F. Sansoz, T. LaGrange, R. T. Ott, J. Marian, T. W. Barbee, Jr., and A. V. Hamza, Nat. Mater. **12**, 697 (2013).

[34] J. W. Cahn, Y. Mishin, and A. Suzuki, Acta Mater. **54**, 4953 (2006).

[35] J. W. Cahn and J. E. Taylor, Acta Mater. **52**, 4887 (2004).

[36] T. J. Rupert, D. S. Gianola, Y. Gan, and K. J. Hemker, Science **326**, 1686 (2009).

[37] Y. Zhang, J. A. Sharon, G. L. Hu, K. T. Ramesh, and K. J. Hemker, Scr. Mater. **68**, 424 (2013).

[38] G. Jyoti, K. D. Joshi, S. C. Gupta, S. K. Sikka, G. K. Dey, and S. Banerjee, Philos. Mag. Lett. **75**, 291 (1997).

[39] D. Milathianaki, S. Boutet, G. J. Williams, A. Higginbotham, D. Ratner, A. E. Gleason, M. Messerschmidt, M. M. Seibert, D. C. Swift, P. Hering, J. Robinson, W. E. White, and J. S. Wark, Science **342**, 220 (2013).